Fully-Plastic Strain-Based *J* Estimation Scheme for Circumferential Surface Cracks in Pipes Subjected to Reeling

Luís F. S. Parise[1]
Department of Naval Architecture and Ocean Engineering,
University of São Paulo,
São Paulo, SP 05508-900, Brazil
e-mail: luis.parise@usp.br

Claudio Ruggieri
Department of Naval Architecture and Ocean Engineering,
University of São Paulo,
São Paulo, SP 05508-900, Brazil
e-mail: claudio.ruggieri@usp.br

Noel P. O'Dowd
Department of Mechanical, Aeronautical and Biomedical Engineering,
Materials and Surface Science Institute,
University of Limerick,
Castletroy, Co.,
Limerick, Ireland
e-mail: Noel.ODowd@ul.ie

Modern installation techniques for marine pipelines and subsea risers are often based on the reel-lay method, which introduces significant (plastic) strains on the pipe during reeling and unreeling. The safe assessment of cracklike flaws under such conditions requires accurate estimations of the elastic–plastic crack driving forces, ideally expressed in a strain-based formulation to better account for the displacement controlled nature of the reeling method. This paper aims to facilitate such assessments by presenting a strain-based expression of the well-known Electric Power Research Institute (EPRI) estimation scheme for the J *integral, which is directly based upon fully plastic descriptions of fracture behavior under significant plasticity. Parametric finite element simulations of bending of circumferentially cracked pipes have been conducted for a set of crack geometries, pipe dimensions, and material hardening properties representative of current applications. These provide the numerical assessment of the crack driving force upon which the nondimensional factors of the EPRI methodology, which scale* J *with applied strain, are derived. Finally, these factors are presented in convenient graphical and tabular forms, thus allowing the direct and accurate assessment of the* J *integral for circumferentially cracked pipes subjected to reeling. Further results show that crack driving force values estimated using the proposed methodology and the given g_1 factors are in very close agreement to those obtained directly from the finite element simulations.*
[DOI: 10.1115/1.4028111]

1 Introduction

The reel-lay method [1] is widely employed by the offshore industry for the installation of subsea pipelines and risers. This method allows the pipeline to be fabricated at onshore facilities by girth welding shorter tubular sections to one another until the entire pipe is formed. Once completed the pipeline is spooled onto a reel which is transported to the location where it is to be installed. The pipeline is then launched to the sea by unspooling the reel, an operation during which the pipe passes through an aligner and a straightener, as shown in Fig. 1(*a*). Figure 1(*b*) illustrates schematically the strain history imposed on the outermost fiber of the pipe during this complete cycle. Point 1 on the figure corresponds to the end of the reeling stage, when the pipe is bent around the reel. Point 2 corresponds to the free span between the reel and the aligner, when the pipe undergoes a reverse deformation and becomes almost straight. Point 3 represents the pipe being bent once again, this time around the aligner. Finally, point 4 represents the effect of the straightener, which induces compressive strains of sufficient magnitude to eliminate any residual deformation when the pipe is deployed to the sea.

When pipes such as medium diameter rigid steel risers undergo reeling deformation they experience large strains, often in the region of 1.5%–3.5%, which is well beyond the material's yielding limits. The safe and accurate assessment of defects is of paramount importance for such highly loaded structures. However, the occurrence of large scale plasticity significantly complicates the evaluation of the pipeline's structural integrity in the presence of defects. The engineering critical assessment (ECA) procedures currently recommended by structural integrity and fitness-for-service (FFS) codes and standards (e.g., BS 7910 [2], API 579 [3]) are based on the assumption that the structural problem under analysis is load-controlled, and that stresses acting on the component can be determined from the applied loading. However, pipeline reeling is a displacement controlled process, which means that the loads acting on the component are often not known explicitly and are caused by the imposed displacements. If bending moment—strain relationships are known for the specific configuration being considered the traditional load based ECA procedures may be used, but they still suffer from certain drawbacks. First, they often do not account explicitly for the possibility of occurrence of large scale plasticity, and their corrections and allowance margins for small scale, contained plasticity might lead to errors or excessive conservatism when extrapolated to the levels of strain commonly found in reeling applications [4]. Second, they present a problem which is illustrated in Fig. 2. Notice, in this figure, how the crack driving force (in this case quantified by the *J* integral) is related to the applied strain through a simple, almost linear relationship over the range of strains typically imposed by reeling procedures, while the relationship between *J* and the bending moment is more complex, having a linear region at low loading levels but then showing a sharp increase in slope at strain levels typical of reeling. Under these conditions, even small errors in the calculation of applied loads can lead to very large errors in the estimation of crack driving forces, potentially compromising the accuracy of traditional load based ECA procedures under significant plasticity. There are, therefore, advantages to be gained from the development of strain-based methodologies for crack driving force estimation applicable to reeling of pipelines.

This has motivated significant amounts of work during the last decade. Most notably, Nourpanah and Taheri [5] have published a simple and accurate *J* estimation scheme for reeled pipes based on a reference strain formulation which builds upon earlier work by Ainsworth [6], who originated the reference stress approach for *J* estimation, and by Linkens et al. [7], who provided a simplified

[1]Corresponding author.

Contributed by the Pressure Vessel and Piping Division of ASME for publication in the Journal of Pressure Vessel Technology. Manuscript received June 24, 2013; final manuscript received July 26, 2014; published online February 23, 2015. Assoc. Editor: Allen C. Smith.

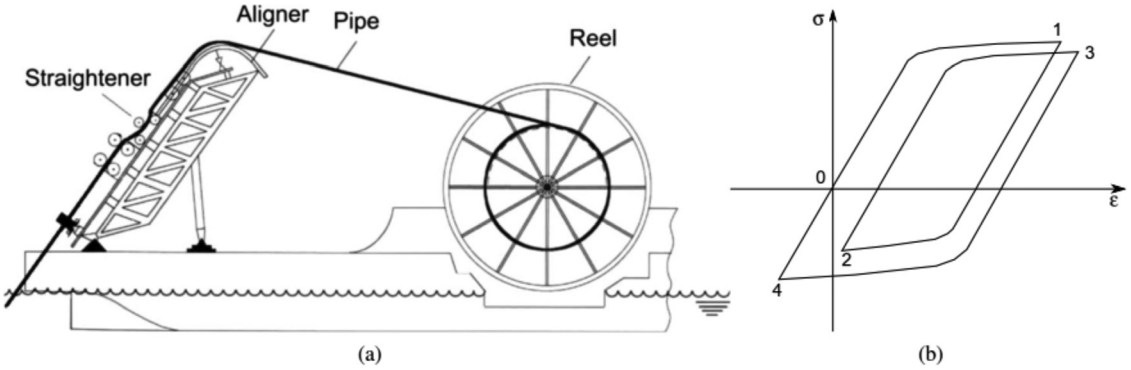

Fig. 1 Pipeline reeling procedure. (*a*) Schematic view [1]. (*b*) Corresponding strain history.

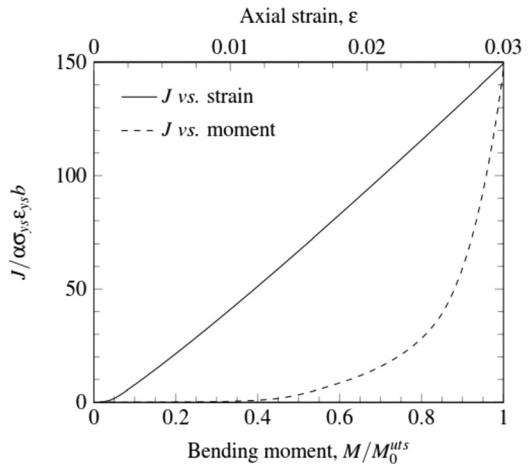

Fig. 2 Evolution of normalized *J* against applied bending moment (normalized by moment corresponding to the tensile strength, M_0^{uts}), and applied axial strain for a typical circumferentially cracked pipe

conversion of this approach to a strain-based formulation. Additionally, Tkaczyk et al. [8] have published a modified reference stress solution which extends the basic approach to cases of displacement control, Budden [4] and Budden and Ainsworth [9] have worked on the development of strain-based failure assessment diagrams (FAD) and Jayadevan, Østby, Thaulow, Hellesvik, and other researchers from SINTEF have published extensive experimental results on the correlation between axial strain and fracture response for pipes subjected to several different loading conditions, e.g., [10–12].

The aforementioned procedures are based on the reference stress approach, which itself is an approximate methodology for *J* estimation, developed from a modification of the EPRI methodology [13], which derives directly from the theoretically rigorous description of fracture response under fully plastic conditions. The reference stress approach sacrifices some accuracy in exchange for general applicability. Chiodo and Ruggieri [14] have shown that the EPRI methodology can be employed very successfully to the estimation of *J*, as well as CTOD (crack tip opening displacement, an alternative measure of fracture toughness and fracture driving force), for circumferentially cracked pipes subjected to bending when bending moment is known. This paper extends the approach to a strain-based formulation and aims to combine the advantages of the work of Nourpanah and Taheri [5] and Chiodo and Ruggieri [14] by developing a strain-based estimation scheme for *J* applicable to the problem of pipeline reeling which is derived directly from fully plastic expressions of nonlinear fracture behavior.

2 Strain-Based *J* Estimation Procedure Derived From Fully Plastic Solutions

2.1 The EPRI Methodology. The elastic–plastic stress–strain behavior of engineering materials may be described through a power-law hardening model of the form

$$\frac{\varepsilon}{\varepsilon_0} = \frac{\sigma}{\sigma_0} + \alpha\left(\frac{\sigma}{\sigma_0}\right)^n \tag{1}$$

which is commonly known as the Ramberg–Osgood (R–O) model. Here, ε denotes the strain, σ represents the stress, σ_0 and ε_0 are normalizing stresses and strains, respectively, n denotes the strain hardening exponent, and α is an additional fitting coefficient. If the assumption is made that, in situations where significant plasticity occurs, the elastic strains (ε_e) are negligible when compared to the plastic strains (ε_p), the model given by Eq. (1) reduces to a pure power-law model of the form $\varepsilon_p \propto \alpha(\sigma/\sigma_0)^n$.

Kumar et al. [13] proposed a procedure to estimate the *J* integral directly based on the assumption of fully plastic conditions described above. This procedure has become widely employed and is known as the EPRI methodology. *J* is decomposed into its elastic (J_e) and plastic (J_p) components according to

$$J = J_e(a) + J_p(a,n) \tag{2}$$

where a is the crack length. The elastic component is obtained from the linear elastic stress intensity factor by

$$J_e = \frac{K_I^2}{E'} \tag{3}$$

where K_I is the Mode I stress intensity factor, E is Young's modulus and $E' = E$ for plane stress or $E' = E/(1-\nu^2)$ for plane strain, ν being the Poisson coefficient. J_e can, therefore, be calculated immediately using any of the many compendia of stress intensity factor solutions which include circumferential surface cracks in cylindrical geometries, e.g., [2,3,15,16].

Estimation of J_p, in turn, is carried out by expressing the proportionality between *J* and remote loading under fully plastic conditions through the expression

$$J_p = \alpha\varepsilon_0\sigma_0 b h_1(a/W, \mathfrak{Q}, n)\left(\frac{P}{P_0}\right)^{n+1} \tag{4}$$

where W is the structural component width, $b = W - a$ denotes the remaining uncracked ligament, $\mathfrak{Q}$ represents additional dependencies on geometry, P is the generalized applied loading and P_0 is a generalized limit load. Finally, h_1 is a nondimensional factor dependent on component dimensions, crack geometry and material behavior which scales the *J* integral with the normalized

applied loading. Once the h_1 factor for the configuration of interest is known, J_p can be readily estimated using Eq. (4) and the total J is then found according to Eq. (2). Kumar et al. [13] and later Zahoor [17] have given solutions of the parameter h_1 for a number of configurations; however, these still remain relatively limited. Solutions for circumferentially cracked pipes under bending have been developed by Chiodo and Ruggieri [14].

2.2 A Strain-Based Version of the EPRI Equation. Recalling that, under fully plastic conditions, the R–O model reduces to the form

$$\frac{\varepsilon}{\varepsilon_0} = \alpha\left(\frac{\sigma}{\sigma_0}\right)^n \tag{5}$$

which implies $\sigma \propto \varepsilon^{1/n}$ and considering, in addition, the result known as Ilyushin's theorem [18], which shows that the fully plastic stresses hold a proportional relationship to the remote applied loading of the form $\sigma = fP$, where f is a nondimensional function of spatial position and material hardening, J can be written in the form of the EPRI estimation framework as

$$J_p = \alpha\varepsilon_0\sigma_0 b g_1(a/W, \mathfrak{L}, n)\left(\frac{\varepsilon}{\varepsilon_0}\right)^{\frac{n+1}{n}} \tag{6}$$

where g_1 is now the nondimensional factor which scales J_p with applied strain. Note that when the estimation equation for J_p is formulated in terms of strain it is not necessary to calculate explicitly any limit or reference load. Also, for large n, $(n+1)/n \rightarrow 1$ so J_p is practically linearly proportional to strain. Even for a relatively low value of n, such as 5, which is typical of a high hardening steel, $(n+1)/n$ still evaluates to just 1.2. This linear relationship has been noted, for example, by Linkens et al. [7] and Nourpanah and Taheri [5], and is one of the basic simplifying assumptions of their methods, as well as of other estimation schemes which correlate J and strain. The EPRI methodology, however, maintains the slightly more accurate original form of the relationship.

Arguing that under fully plastic conditions, and certainly in the strain range typical of pipeline reeling, the plastic component of strain, ε_p, is much larger than the elastic component, ε_e, and also that the single term on the right hand side of the reduced R–O model given by Eq. (5) actually better represents the plastic rather than total strain, Eq. (6) can be rewritten in terms of ε_p as

$$J_p = \alpha\varepsilon_0\sigma_0 b g_1(a/W, \mathfrak{L}, n)\left(\frac{\varepsilon_p}{\varepsilon_0}\right)^{\frac{n+1}{n}} \tag{7}$$

As will be shown later, this modified equation improves the accuracy of J estimations made using the methodology derived here. It is, therefore, the recommended equation to be used for calculation of J_p.

2.2.1 Extension to Circumferentially Cracked Pipes Under Pure Bending. Figure 3 shows the relevant pipe and crack dimensions for typical circumferentially cracked pipes subjected to pure bending. Considering the nondimensional ratios of these parameters which affect the value of the g_1 factor, Eq. (6) can be rewritten for this particular case as

$$J_p = \alpha\varepsilon_0\sigma_0 b g_1(a/t, \theta/\pi, D/t, n)\left(\frac{\varepsilon_p}{\varepsilon_0}\right)^{\frac{n+1}{n}} \tag{8}$$

where t is the pipe wall thickness, the uncracked ligament is now $b = t - a$, θ is the angular measurement of the crack length, given by [3,17]

$$\theta = \frac{\pi c}{2D} \tag{9}$$

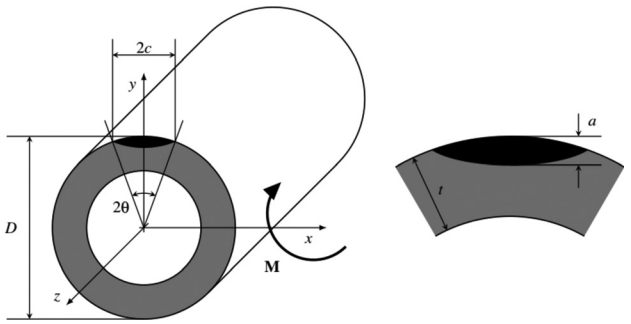

Fig. 3 Schematic illustration of the pipe configuration, crack geometry, and pure bending loading considered in the numerical analyses

and D is the outer diameter of the pipe. In Eq. (9), c is the crack half length. It is important to note that the normalized crack length calculated by Eq. (9) does not actually correspond exactly to the schematic illustration of Fig. 3. This formula has been chosen for consistency with the fundamental publications upon which this research is based, namely, the extended EPRI methodology report by Zahoor [17] and the API 579 standard [3]. The crack length thus calculated is slightly larger than the one obtained by the exact arc length formula $c = \theta(D/2)$. This will not affect the accuracy of J estimations carried out according to this procedure, provided the analyst also uses Eq. (9) to calculate θ for the crack being evaluated and then selects the appropriate value for the g_1 factor, according to the compendia given in the results section of this text.

In Eq. (8) above, the plastic strain ε_p is now particularized to the global (not influenced by the presence of the crack) longitudinal plastic strain acting on the outermost fiber of the pipe. In the case of a reeling application, this strain can be calculated by

$$\varepsilon_p = \frac{D/2}{R + D/2} - \frac{\sigma}{E} \tag{10}$$

The first term on the right hand side of Eq. (10) represents the total axial strain, ε, calculated as a function of pipe and reel dimensions (R is the reel radius) [19]. The second term is the elastic strain, which in order to be calculated requires that the total axial stress, σ, be known. This stress can be found by a very straightforward numerical approximation procedure which simply determines the stress that corresponds to a given strain, in this case the total strain, on the Ramberg–Osgood equation. Alternatively, σ can also be calculated from ε by using approximate analytical inverse forms of the R–O stress–strain relationship, such as the one developed by Mostaghel and Byrd [20]. The strain-based equation proposed here, therefore, allows the estimation of the J integral even if the applied loads are not explicit known, which is usually the case in displacement controlled problems.

Calculation of J_e, in turn, is carried out using Eq. (3). The FFS standard API 579 [3] provides recently developed and improved stress intensity factor solutions for circumferential surface cracks in cylinders. For pure bending, the solution is given in the form

$$K_I = G_5\sigma\sqrt{\frac{\pi a}{Q_s}} \tag{11}$$

where G_5 is an influence coefficient whose precise calculation is detailed in the standard, Q_s is the flaw shape parameter, defined as

$$Q_s = 1 + 1.464\left(\frac{a}{c}\right)^{1.65}, \quad a \geq c \tag{12}$$

and σ is the total axial stress, obtained directly from the total strain using simple numerical approximations, as discussed above.

3 Computational Procedures

3.1 Finite Element Models. A series of parametric finite element simulations of circumferentially cracked pipes subjected to pure bending have been conducted. The pipe radial dimension is described by the nondimensional D/t ratio, where D is the outer diameter and t is the wall thickness. The finite element models developed for the numerical analyses have wall thickness $t = 20.6$ mm and outer diameters $D = 206$ mm ($D/t = 10$) and $D = 412$ mm ($D/t = 20$). Five crack depths (a) and three crack lengths ($2c$) are considered in the analysis matrix. The normalized depth has been varied from $a/t = 0.1$ up to $a/t = 0.5$ in increments of 0.1 and the normalized lengths have been chosen as $\theta/\pi = 0.04$, 0.12, and 0.20, which correspond to a/c ratios in the range $0.0125 \le a/c \le 0.625$. Figure 3 illustrates the geometrical features of the pipe and crack represented in the models.

Figure 4 shows a typical finite element model developed for the numerical analyses. Hexahedral eight node elements have been used throughout the entire model and a focal mesh with ten concentric rings has been constructed around the crack tip (Fig. 4(*c*)), with the smallest element dimensions being on the order of 10^{-2} mm. The elements of the first ring have two coincident edges at the crack tip, thus forming what are known as degenerate elements with a wedge shape along the crack front. This makes the crack ideally sharp initially, but allows it to blunt as deformation advances. The developed models all have between 10,000 and 15,000 elements and between 12,000 and 18,000 nodes, depending on the particular combination of pipe dimension and crack geometry. Previous mesh studies by the authors have shown this level of discretization and choice of element order to be sufficiently accurate for the current analysis purposes.

Appropriate constraints are imposed along both symmetry planes so that only one quarter of the cracked pipe needs to be modeled. A reference point is defined at the free end of the model and connected to all nodes at that end using multipoint constraints, as shown in Fig. 4(*a*). Pure bending is then applied by imposing a rotation to the reference point, calculated so as to generate a maximum longitudinal strain slightly greater than 3.5%. Although this level of strain is larger than what is currently seen in typical rigid pipeline reeling applications, it was judged interesting to extend the evaluated strain range up to this level, so as to make the results obtained applicable to a wider class of strain-based problems and also anticipating possible future trends toward larger strains in reeling. The relationship between the reference node rotation and the longitudinal strain at the outermost fiber of the pipe is given by the relation

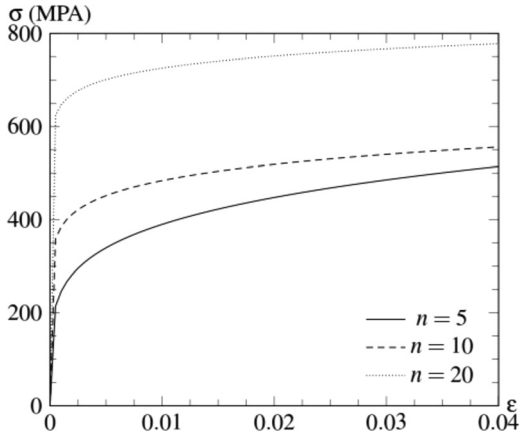

Fig. 5 Stress–strain curves for the different materials analyzed in the finite element models (shown up to 4% strain only)

$$\psi = \frac{2\varepsilon L}{D} \tag{13}$$

where ψ is the angle of rotation and L is the model length. Equation (13) is determined directly from geometric considerations. A vertical support boundary condition is also defined at the reference point so that the model cannot undergo any rigid body motions.

3.2 Material Models. The constitutive model employed in the analyses follows a J_2 (Mises) deformation plasticity theory under small geometry change (SGC) assumptions. Following previous studies [14,21], three different materials were modeled, with mechanical behavior representative of current trends in high, medium, and low strain hardening structural and pipeline steels. All three materials have Young's modulus $E = 206$ GPa, the high hardening material has hardening exponent $n = 5$ and a yield

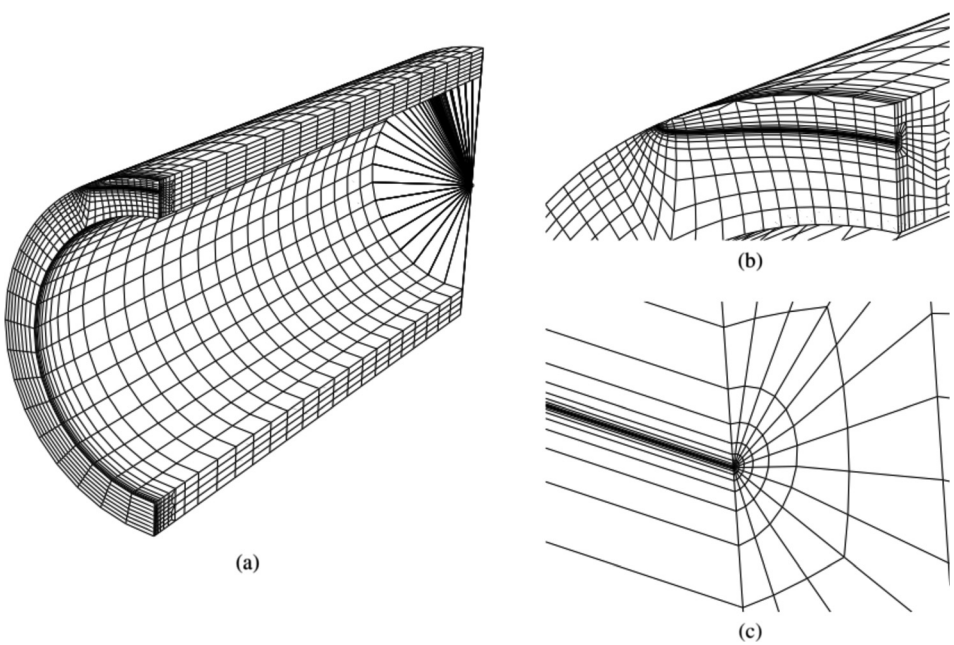

Fig. 4 Typical finite element model employed in the computational simulations: (*a*) Pipe mesh and rigid link at the remote end; (*b*) detail of the crack region; and (*c*) crack tip mesh.

Table 1 g_1 factors for the pipe with $D/t = 10$ and the different crack geometries and material strain hardening levels analyzed

		g_1				
n	θ/π	$a/t = 0.1$	$a/t = 0.2$	$a/t = 0.3$	$a/t = 0.4$	$a/t = 0.5$
5	0.04	0.5325	1.233	2.134	3.153	4.273
	0.12	0.5944	1.705	3.861	7.539	12.75
	0.20	0.5968	1.809	4.449	9.772	19.38
10	0.04	0.6145	1.466	2.627	3.987	5.536
	0.12	0.7119	2.194	5.416	10.97	19.00
	0.20	0.7214	2.411	6.793	16.45	36.40
20	0.04	0.6977	1.718	3.191	5.008	7.138
	0.12	0.8397	2.813	7.670	16.14	30.83
	0.20	0.8614	3.248	10.85	30.14	84.29

stress of $\sigma_{ys} = 257$ MPa ($E/\sigma_{ys} = 800$), the medium hardening material has $n = 10$ and $\sigma_{ys} = 412$ MPa ($E/\sigma_{ys} = 500$), and the low hardening material has $n = 20$ and $\sigma_{ys} = 687$ MPa ($E/\sigma_{ys} = 300$). The α coefficient of the R–O model is set equal to unity for all three materials. In particular, the behavior of the material with $n = 10$ is in line with what is observed for many pipeline steels of grade API 5L X60 to X65 [22], whereas the material with $n = 20$, which has higher yield strength but lower strain hardening capacity, would better represent pipeline steel grades such as API 5L X80 or above [22]. Figure 5 shows the stress–strain curves for the three materials considered over the strain range adopted in the computational analyses.

3.3 Solution Procedures. The analyzed finite element models were developed and processed using the ABAQUS software, version 6.11. The eight-node, fully integrated hexahedral elements used are designated by the code C3D8 in the software. The multipoint constraint which links the nodes at the free end of the pipe with the reference point is of the predefined "beam" type. The J integral is calculated using a domain integral method [23] and the J value used for calibration of the nondimensional g_1 factors was the average of the values calculated for each of the ten rings of elements of the focal mesh, excluding the one immediately surrounding the crack tip, which is considered inaccurate. Confidence about the path independence of the numerical J values was gained by noting that their standard deviation throughout the nine considered rings was within 4% of the average J for all analyzed models. Confidence in the accuracy of the numerical J values obtained was also increased by comparing them with results from similar simulations carried out previously by Chiodo and Ruggieri [14] and Parise and Ruggieri [21] using the WARP3D [24] finite element software and noting that they presented very good agreement. The yield strength values of the three materials considered were used as the normalizing parameters when describing the constants of the deformation plasticity model in Abaqus. Therefore, the yield strength, σ_{ys}, and corresponding strain, ε_{ys} should be used to particularize σ_0 and ε_0 in Eq. (8) when using the g_1 factors given in Sec. 4 to estimate J.

4 Results

4.1 Nondimensional g_1 Factors for J Estimation. Determination of the J integral according to the procedure outlined previously, all other quantities being known by the analyst, requires that the g_1 factor for the configuration of interest be given, so that J_p can be calculated from the applied strain and material properties. Table 1 and Fig. 6 present the results obtained for g_1 factors for the pipe with diameter $D/t = 10$ calibrated from the finite

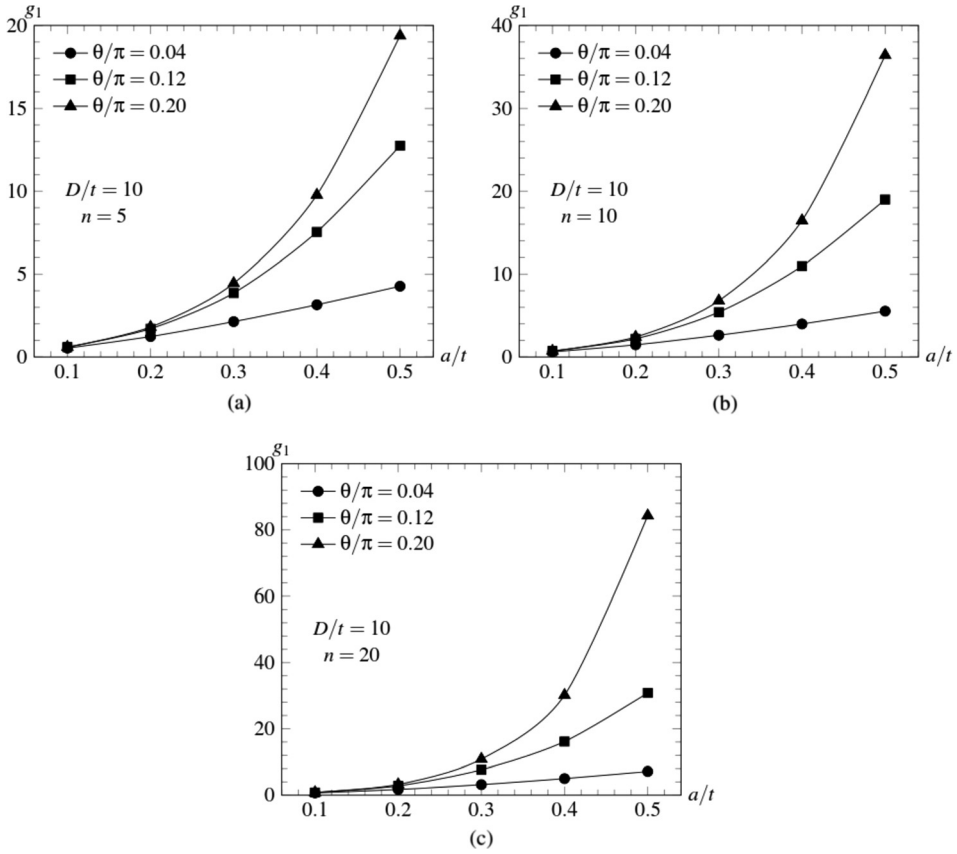

Fig. 6 Variation of g_1 with normalized crack depth and length for $D/t = 10$: (a) $n = 5$; (b) $n = 10$; and (c) $n = 20$

Table 2 g_1 factors for the pipe with $D/t = 20$ and the different crack geometries and material strain hardening levels analyzed

		g_1				
n	θ/π	$a/t = 0.1$	$a/t = 0.2$	$a/t = 0.3$	$a/t = 0.4$	$a/t = 0.5$
5	0.04	0.5813	1.599	3.373	5.983	9.466
	0.12	0.6208	2.014	5.348	12.33	23.94
	0.20	0.6137	2.023	5.713	14.54	32.32
10	0.04	0.6887	2.012	4.538	8.155	12.86
	0.12	0.7597	2.801	8.710	21.00	42.48
	0.20	0.7526	2.877	10.23	29.48	76.35
20	0.04	0.7985	2.503	6.091	11.02	18.06
	0.12	0.9130	3.959	14.82	37.20	88.06
	0.20	0.9066	4.256	20.58	70.77	245.4

element analyses described in Sec. 3. Table 2 and Fig. 7 present the g_1 factors for the pipe with $D/t = 20$.

The nondimensional factors presented here have been calculated by plotting $\overline{J_p} = J_p/\alpha\varepsilon_{ys}\sigma_{ys}b$ against $\varepsilon = (\varepsilon_p/\varepsilon_{ys})^{(n+1)/n}$ for each step of the finite element solution and fitting a straight line to the plotted data using a least squares method. The fitting line is required to pass through the origin in order to account for the necessary condition that J_p be zero when ε_p is zero. Any points for which $\varepsilon < \varepsilon_{ys}$ are excluded from the regression and the value of g_1 for each particular configuration is then the slope of this line. This procedure is illustrated for a typical case in Fig. 8, which shows that J_p can indeed be accurately represented as a function of strain by the relation proposed in this paper (Eq. (7)).

While Tables 1 and 2 present the data in a numerical form which facilitates interpolation for any configuration within the limits of the analysis matrix (linear interpolation will tend to yield conservative estimates), it is easier to visualize the effect of the

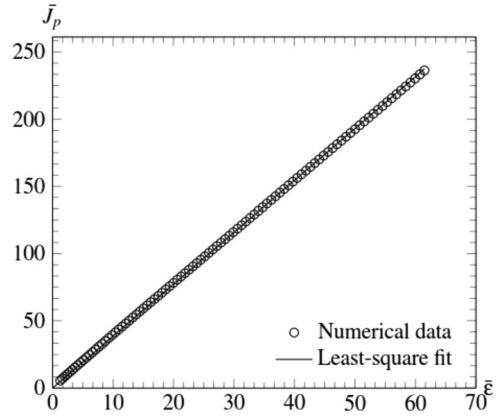

Fig. 8 Illustration of g_1 factor calculation procedure based on linear regression over numerical data. $D/t = 10$, $a/t = 0.3$, $\theta/\pi = 0.12$, $n = 5$

ratios a/t and θ/π, as well as the pipe diameter and strain hardening level on the g_1 factors by considering Figs. 6 and 7. It can be seen that, in all cases θ/π has virtually no effect on g_1 for the shallower cracks ($a/t = 0.1$ and 0.2), a transition then occurs around $a/t = 0.3$ and the effects become quite pronounced for the deeper cracks ($a/t = 0.4$ and 0.5). This can be seen in any given graph by noting the increasing separation between the curves as crack depth increases. According to what would be expected intuitively the longest cracks are always associated with the highest g_1 values (higher J for a given level of strain and crack depth) and the shortest cracks always give rise to the lowest g_1 factors (lowest J for a given level of strain and crack depth). The effect of the a/t ratio over g_1 is seen to be that of increasing the value of the

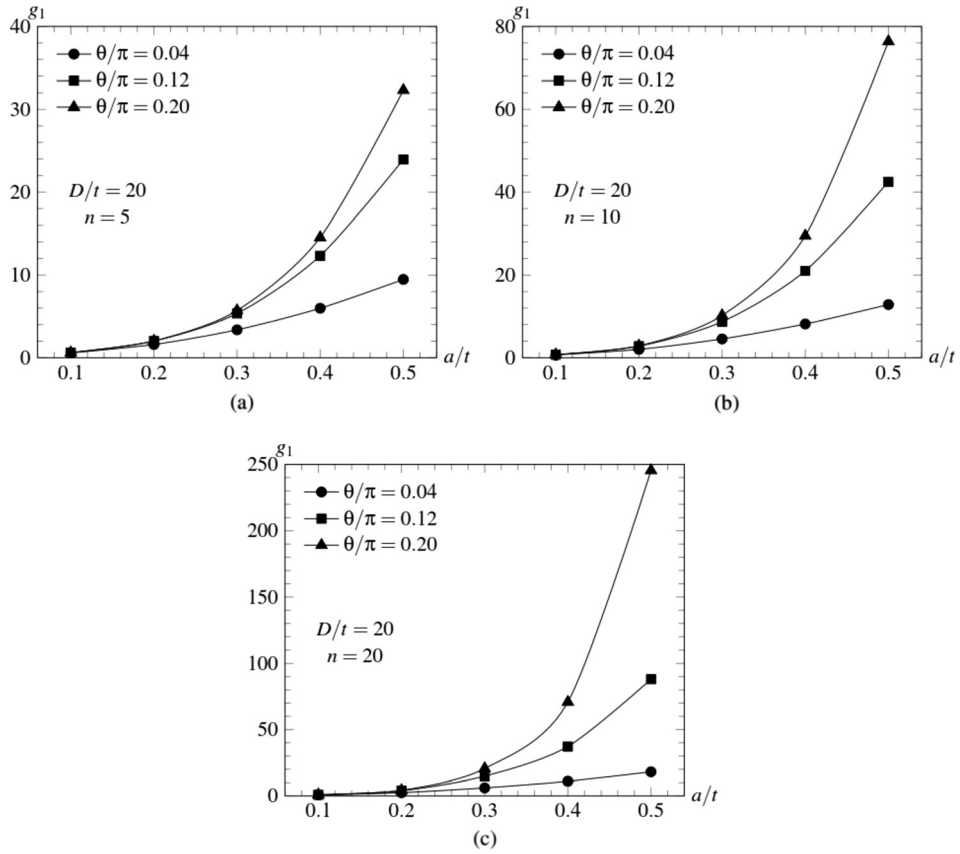

Fig. 7 Variation of g_1 with normalized crack depth and length for $D/t = 20$: (a) $n = 5$; (b) $n = 10$; and (c) $n = 20$

nondimensional factor as the crack depth increases, which is also consistent in all cases with what would be expected intuitively. Deeper cracks, all else remaining equal, cause larger values of J. Note, however, that the increase in g_1 with crack depth is much more pronounced for longer cracks than for shorter ones. Also, the increase is particularly small for the combination of short crack ($\theta/\pi = 0.04$) and low hardening. The pipe diameter is seen to have a quantitative but not qualitative effect on the behavior of g_1 factors. Finally, the strain hardening exponent is seen to have a rather significant effect on g_1, with low hardening leading to particularly large values.

4.2 Preliminary Validation. As an illustrative preliminary validation of the strain-based procedure for J estimation presented here, Fig. 9 shows the evolution of J with applied strain as obtained directly from numerical simulations and as estimated using the calculated g_1 factors and Eq. (7). Figure 9 refers to the pipe with $D/t = 20$ containing a crack with depth $a/t = 0.3$, length $\theta/\pi = 0.12$ and moderate hardening material. For purposes of comparison, the figure also presents an estimation of J carried out using Eq. (6), which is based on total rather than plastic strain, and appropriate g_1 factors for that expression. Comparing the curves on these plots shows that the proposed methodology presents excellent agreement to the finite element results over the entire strain range evaluated. This agreement is a result of expressing the J_p estimation equation as a function of ε_p. When the total strain, ε, is considered instead, it can be seen that the agreement obtained is not as close. Furthermore, J estimates obtained from Eq. (6) are nonconservative for strains greater than 2%. Therefore, Eq. (7) is seen to be a clearly superior formulation. For materials with higher strain hardening and for shorter/shallower cracks, the differences between both formulations are less pronounced.

4.3 Minimum Allowable Reel Diameter Calculation. Beside presenting an analytical expression for the strain based estimation of the J integral for reeled pipes and providing the set of nondimensional g_1 factors required by this expression, the present work also gives analysts a practical tool to quickly estimate the minimum allowable reel dimension for a given reeling procedure. If the material's fracture toughness is known and the dimensions of a crack found on the pipe have been well characterized, the estimation procedure presented previously can be used in reverse order to calculate the longitudinal strain corresponding to the maximum allowable value of J. The reel radius corresponding to this strain can then be determined.

As an example of this reverse use of the proposed methodology, consider the illustrative problem in which a steel pipeline with $D/t = 10$ is being reeled. Suppose that a crack with $a/t = 0.3$ and

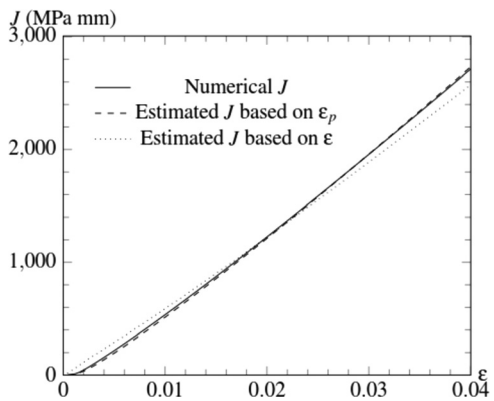

Fig. 9 Comparative evolution of J with applied strain as calculated from finite element analyses and as estimated using g_1 factors. $D/t = 20$, $a/t = 0.3$, $\theta/\pi = 0.12$, $n = 10$

$\theta/\pi = 0.12$ has been detected on it. Consider also that a typical fracture toughness J_c for an API 5L X60/X70 grade pipeline steel is on the order of 400 MPa mm and (for illustrative purposes only) that the plastic component of J must not be allowed to exceed 80% of this value. Equation (8) can be rewritten as

$$\varepsilon_p = \varepsilon_0 \left(\frac{J_p}{\alpha \sigma_0 \varepsilon_0 b g_1} \right)^{\frac{n}{n+1}} \tag{14}$$

Substituting the values $\varepsilon_0 = 0.002$, $J_p = 320$ MPa mm, $\alpha = 1$, $\sigma_0 = 412$ MPa, $b = 14.42$ mm, $g_1 = 5.416$, and $n = 10$ on the previous expression gives $\varepsilon_p = 0.0086$. Iterating over a range of values for the reel radius and replacing these values, along with ε_p, in Eq. (10) until a sufficiently close approximation is found then gives a reel radius of $R \approx 9.3$ m. Therefore, employing a reel with radius equal or superior to this value on the reeling procedure will ensure that the driving force for the analyzed crack does not exceed its allowed limit.

5 Discussion

Chiodo and Ruggieri have shown in previous research [14] that when the EPRI methodology is extended to pipes subjected to bending under the traditional load based framework the results obtained are not reliable for deep and long cracks when the material exhibits low hardening ($n = 20$). The range of validity is then limited to $a/t \leq 0.25$ and $\theta/\pi \leq 0.12$. Beyond these limits the proportionality between J and bending moment is only verified at unrealistically high loads. Since a proportional relationship between J and global loading is one of the fundamental concepts which allow the EPRI estimation scheme to be derived from fully plastic solutions the methodology has been considered inadequate to evaluate J for deep and long cracks in pipes with low strain hardening. Their research shows that the methodology is accurate for all other combinations of crack, pipe, and material evaluated. In the research reported in this paper, J_p and ε have been found to follow the $(n+1)/n$ proportionality slope for the entire range of strain evaluated, even when large (deep/long) cracks are combined with low hardening materials. This does not mean, however, that the methodology and results described here should be used indiscriminately in the analysis of reeled pipes. Indeed, the very sharp increase in g_1 values (and hence in the J integral) which happens for the $n = 20$ material when the crack is deep and long indicates that such configurations must be treated with great caution. Although this behavior is consistent with experimental results published by Østby et al. [11], which show that fracture response (in their research quantified by the CTOD) increases very abruptly with little applied strain for deep cracks in moderate to low hardening pipes, it must be kept in mind that what this really indicates is that when large cracks are present such pipes most likely cannot actually be reeled to strains in the region of, for example, 2–3.5% without leading to the unstable growth of the cracks and subsequent structural collapse.

The simulations reported here have been carried out under certain simplifying assumptions, most notably the SGC (small strain) formulation coupled to a deformation plasticity model. If complex nonlinear analyses are carried out to validate the results it may be found that in certain severe cases crack propagation will occur before the final strain level is reached or the almost linear proportionality between J and strain implied and required by the EPRI-like equation developed previously will be lost before the target strain of the case being evaluated is reached. These more complex analyses might include features such as a finite strain formulation, incremental plasticity material model, algorithmic capacities to account for possible crack growth, and contact of the pipe with a rigid cylindrical surface representing the reel. Validations of this type will be dealt with in future work, although for the majority of analyzed cases results are not expected to be significantly different from those already obtained. Also, for yet another set of cases

it may be the case that competing failure modes, such as buckling of the compressed side of the pipe or excessive ovalization of the cracked cross section may occur at some strain level of interest, even if the structure remains safe from a fracture point of view. Conclusions about this can also be drawn from less simplified numerical validations.

6 Summary and Conclusion

This work outlines a strain-based procedure which is directly derived from fully plastic descriptions of fracture behavior under large scale yielding conditions to estimate the J integral in circumferentially surface cracked pipes subjected to reeling, as well as presents initial results in terms of nondimensional g_1 factors which relate J to applied strain. The strain-based nature of the outlined procedure allows the J integral to be determined without requiring explicit knowledge of the applied loading or calculation of normalizing or reference loads. It also takes advantage of the accuracy provided by the almost linear relationship that exists between J and longitudinal strain for the strain levels commonly found in reeling applications. This avoids the abrupt change in slope seen in the relationship between J and global loading that could lead to large errors in the load based estimation of the crack driving force if even small errors are made when calculating the loads.

Acknowledgment

The financial support of the Brazilian National Council for Scientific and Technological Development is gratefully acknowledged. The University of Limerick and the Science Without Borders program are acknowledged for facilitating this Brazilian-Irish cooperation. The ASME 2013 Pressure Vessels and Piping Conference is acknowledged as the original publisher of this research paper, which appears in the proceedings of that conference as PVP2013-97794. The version presented here has been slightly modified, updated and corrected.

Nomenclature

a = crack depth
b = remaining ligament
c = crack half length
D = pipe outer diameter
E = Young's modulus
E' = "effective" Young's modulus under plane stress/plane strain
g_1 = nondimensional factor correlating J and strain
G_5 = influence coefficient from API 579 standard
h_1 = nondimensional factor correlating J and loading
J = J integral
J_e = elastic component of the J integral
J_p = plastic component of the J integral
K_I = mode I stress intensity factor
L = finite element pipe model length
M_0^{uts} = bending moment corresponding to material's tensile strength
n = material hardening exponent
P = generalized load
P_0 = limit load associated to P
Q_s = flaw shape parameter from API 579 standard
R = reel radius
t = pipe wall thickness
CTOD = crack tip opening displacement
W = component width
α = Ramberg–Osgood fitting parameter
ε = axial strain on pipe outer fiber
ε_0 = reference strain value
ε_p = plastic component of strain
ε_{ys} = strain corresponding to yield strength
θ = angular measure of crack half length
σ = axial stress on pipe outer fiber
σ_0 = reference stress value
σ_{ys} = material yield strength
$\mathfrak{Q}$ = component characteristic dimension
Ψ = finite element model reference node rotation

References

[1] Kyriakides, S., and Corona, E., 2007, *Mechanics of Offshore Pipelines, Vol. 1: Buckling and Collapse*, Elsevier. Available at: http://store.elsevier.com/Mechanics-of-Offshore-Pipelines/Stelios-Kyriakides/isbn-9780080551401/
[2] British Standard Institution, 2005, *Guide on Methods for Assessing the Acceptability of Flaws in Metallic Structures*, Paper No. BS 7910.
[3] American Petroleum Institute, 2007, *Fitness-for-Service*, No. API 579/ASME FFS-1.
[4] Budden, P. J., 2006, "Failure Assessment Diagram Methods for Strain-Based Fracture," Eng. Fract. Mech., **73**(5), pp. 537–552.
[5] Nourpanah, N., and Taheri, F., 2010, "Development of a Reference Strain Approach for Assessment of Fracture Response of Reeled Pipelines," Eng. Fract. Mech., **77**(12), pp. 2337–2353.
[6] Ainsworth, R. A., 1984, "The Assessment of Defects in Structures of Strain Hardening Materials," Eng. Fract. Mech., **19**(4), pp. 633–642.
[7] Linkens, D., Formby, C. L., and Ainsworth, R. A., 2000, "A Strain-Based Approach to Fracture Assessments: Example Applications," 5th International Conference on Engineering Structural Integrity Management, pp. 45–52. Available at: https://getinfo.de/app/A-Strain-Based-Approach-to-Fracture-Assessment/id/BLCP%3ACN039352631
[8] Tkaczyk, T., O'Dowd, N. P., and Nikbin, K., 2009, "Fracture Assessment Procedures for Steel Pipelines Using a Modified Reference Stress Solution," ASME J. Pressure Vessel Technol., **131**(3), p. 031409.
[9] Budden, P. J., and Ainsworth, R. A., 2012, "The Shape of a Strain-Based Failure Assessment Diagram," Int. J. Press. Vessels Pip., **89**, pp. 59–66.
[10] Jayadevan, K. R., Østby, E., and Thaulow, C., 2004, "Fracture Response of Pipelines Subject to Large Plastic Deformation Under Tension," Int. J. Press. Vessels Pip., **81**, pp. 771–783.
[11] Østby, E., Jayadevan, K. R., and Thaulow, C., 2005, "Fracture Response of Pipelines Subject to Large Plastic Deformation Under Bending," Int. J. Press. Vessels Pip., **82**(9), pp. 201–215.
[12] Østby, E., and Hellesvik, A. O., 2008, "Large-Scale Experimental Investigation of the Effect of Biaxial Loading on the Deformation Capacity of Pipes With Defects," Int. J. Press. Vessels Pip., **85**(11), pp. 814–824.
[13] Kumar, K., German, M. D., and Shih, C. F., 1981, "An Engineering Approach to Elastic-Plastic Fracture Analysis," Electric Power Research Institute, Palo Alto, CA, EPRI Report No. NP-1931.
[14] Chiodo, M. S. G., and Ruggieri, C., 2010, "J and CTOD Estimation Procedure for Circumferential Surface Cracks in Pipes Under Bending," Eng. Fract. Mech., **77**(3), pp. 415–436.
[15] Tada, H., Paris, P. C., and Irwin, G. R., 1985, *The Stress Analysis of Cracks Handbook*, 2 ed., Paris Productions, St. Louis, MO.
[16] Marie, S., Chapuliot, S., Kayser, Y., Lacire, M. H., Drubay, B., and Barthelet, B., 2007, "French RSE-M and RCC-MR Code Appendixes for Flaw Analysis: Presentation of the Fracture Parameter Calculation—Part I: General Overview," Int. J. Press. Vessels Pip., **84**(10–11), pp. 590–600.
[17] Zahoor, A., 1989, "Ductile Fracture Handbook," Electric Power Research Institute, Palo Alto, CA, EPRI Report No. NP-6301-D.
[18] Ilyushin, A. A., 1946, "The Theory of Small Elastic Plastic Deformations," Prikadnaia Matematicai Mekhanika, **10**, pp. 347–356 (in Russian).
[19] Det Norske Veritas, 2006, *Offshore Standard–Fracture Control for Pipeline Installation Methods Introducing Cyclic Plastic Strain*. Paper No. DNV-RP-F108.
[20] Mostaghel, N., and Byrd, R. A., 2002, "Inversion of Ramberg-Osgood Equation and Description of Hysteresis Loops," Int. J. Non Linear Mech., **37**(8), pp. 1319–1335.
[21] Parise, L. F. S., and Ruggieri, C., 2011, "J and CTOD Estimation Procedure for Circumferentially Cracked Pipes Under Combined Bending and Internal Pressure," ASME 2011 Pressure Vessels and Piping Division Conference, No. ASME PVP 2011.
[22] American Petroleum Institute, 2000, *API Specification for Line Pipe*. API 5L. Washington, DC. Available at: https://law.resource.org/pub/us/cfr/ibr/002/api.5l.2004.pdf
[23] Simulia-Dassault Systèmes, 2011, *Abaqus Analysis User's Manual, Vol. II: Analysis*.
[24] Healy, B., Gullerud, A., Koppenhoefer, K., Roy, A., RoyChowdhury, S., Walters, M., Bichon, B., Cochran, K., Carlyle, A., Sobo, J., Messner, M., and Dodds, R., 2012, "WARP3D - Release 17.2: 3-D Dynamic Nonlinear Fracture Analysis of Solids Using Parallel Computers," Technical Report, University of Illinois at Urbana-Champaign, Champaign, IL, Civil Engineering Studies, Structural Research Series No. 607.